

Space-Charge-Limited Conduction in Thin Film Al/Sb₂Pb₁Se₇/Al Devices

Shaila Wagle and Vinay Shirodkar

*Solid State Electronics Laboratory, Department of Physics,
The Institute of Science, 15, Madam Cama Road,
Mumbai - 400 032. India*

Received on 20 June, 1999. Revised version received on 10 November 1999

Thin film Al/Sb₂Pb₁Se₇/Al, MGM, sandwiched structures, prepared using thermal evaporation technique have been studied. The DC measurements at low electric field suggest that the electrical transport is governed by space charge limited conduction (SCLC) mechanism. The detailed analysis of current-voltage limited conduction (SCLC) mechanism characteristics on the basis of SCLC theory reveals the presence of uniformly distributed trap density of the order of $10^{23} \text{ m}^{-3} \text{ eV}^{-1}$ with average activation energy 0.48 eV.

I Introduction

Thin film technology is well established and widely used in the fabricating of electronic devices. The technique has been successfully used to fabricate thin film resistors, capacitors, photoelectronic devices etc.[1,2]. The use of this technique in fabricating electronic devices makes it necessary to understand the electrical properties of the material in thin film form.

In the device applications of thin films, new and complex materials are being used and developed and their electrical properties are being studied. The disordered materials, particularly amorphous semiconductors, covering a wide range of compositions and with interesting electrical properties, have been studied in greater detail[3-5]. A good amount of work on the DC conduction of chalcogenide/glassy materials in the form of metal-glass-metal (MGM) structure has been reported by many researchers[3,6]. Since these materials are well known for their property to switch from one impedance state to another, when subjected to high field of the order of 10^6 V/cm , most of the reported work pertains to the electrical measurements carried out at high fields. However, it is equally important to know the behaviour of these materials at low electric fields upto about 10^4 V/cm .

To the best of our knowledge no attempt has been made to study the low field DC conduction of vacuum evaporated Sb₂Pb₁Se₇ thin films. In the present paper therefore, we report on the low field DC measurements carried out to determine the prevalent conduc-

tion mechanism in vacuum deposited Sb₂Pb₁Se₇ films.

II Experimental

The Sb₂Pb₁Se₇ compound used to fabricate the metal-glass-metal, MGM, devices was prepared as follows. Initially, the weighed quantities of high purity (5N) Sb, Pb and Se, taken in their atomic proportions, to give Sb₂Pb₁Se₇ composition, were crushed and mixed together. The mixture was then introduced in a high purity quartz tube closed at one end and made into a neck with constriction at the other end. The quartz ampoule was evacuated to 10^{-5} mbar and filled again with dry argon to increase its pressure to about 10^{-3} mbar. The ampoule was sealed at the point of constriction and introduced in a rocking furnace. The temperature of the furnace was raised to 1100°C and maintained at that level for about five hours. The rocking furnace helped thoroughly to mix the constituents in the quartz ampoule to form the compound. After completion of the reaction the quartz ampoule was allowed to fall directly into a liquid nitrogen container. The ampoule was then broke open and glassy mass thus obtained was crushed into fine powder and stored securely in a dessicator.

The MGM devices were fabricated, on thoroughly cleaned microscope glass slides, using Edwards Co. (UK) Turbomolecular pumping station. The working chamber was fitted with Maxtek (USA) film deposition controller model FDC - 440, which can display film thickness in angstrom units directly if various parameters such as density, acoustic impedance, tooling factor

and many such parameters are fed into the program. The thickness of film was also measured using Dektak thickness profilometer and was found to be within 1% of the displayed value by the FDC - 440. The base plate housed an eight source turret, while the top plate was fitted with mask changer assembly, both of which could be monitored externally without requiring to break the vacuum. The ultimate working pressure during the deposition was 5×10^{-6} mbar. Initially, aluminium metal was evaporated and deposited on the substrate in the form of two parallel strips each 60mm long, 2mm wide and separated by 5mm from each other. These strips formed a pair of lower electrodes. The material was deposited on the strips through an appropriate mask to cover area of 50mm \times 15mm, leaving 5mm of the end portions of each aluminium strip. Six counter electrodes, each 2mm wide and 20mm long, perpendicular to the lower electrodes were deposited on the material to obtain 12 MGM devices each of area 4mm² (see Figs. 1a and 1b). The entire deposition sequence was completed without breaking the vacuum at any stage. This made it convenient repeatedly to carry out all the electrical measurements on a film, of any particular thickness, using twelve devices prepared essentially under identical deposition conditions.

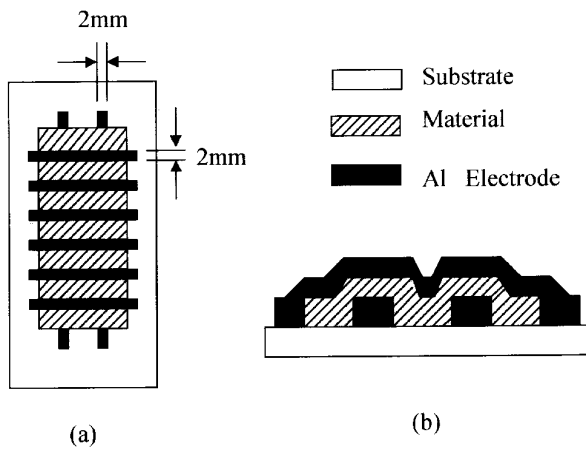


Figure 1. a. Schematic view of metal-glass-metal devices. b. Cross sectional view of the devices.

The electrical measurements on the devices were carried out in vacuum using a cryostat which could be evacuated to 10^{-2} mbar pressure during the measurements. The substrate temperature inside the cryostat could be varied from 150 K to 500 K. The current-voltage, I-V, measurements were carried out using a regulated power supply connected in series with the device under investigation and a standard resistor. The current through the device was calculated by accurately monitoring the potential drop across the standard resistor using Keithley nano-voltmeter model 181, while the

voltage across the device was obtained as a difference between supply voltage and drop across the standard resistor. The series resistor also helped to prevent the flow of excessive current through the device when the supply voltage would overshoot accidentally.

III Results and discussion

Fig. 2, curve 'a', shows a typical room temperature I-V curve of Al/Sb₂Pb₁Se₇/Al sample with film thickness 270 nm. It is seen that the curve exhibits a highly non-linear feature. The non-linearity of the I-V characteristics indicates that the prevalent conduction mechanism is non-ohmic in nature.

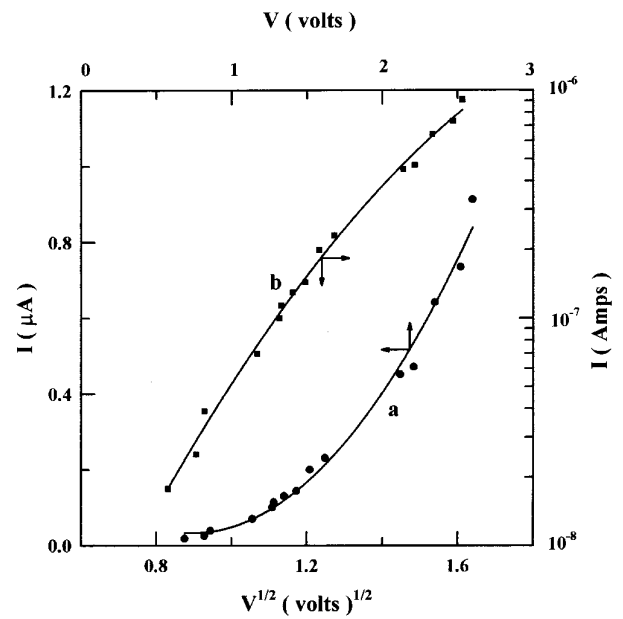


Figure 2. Room temperature I-V. curve a, and $\log I - V^{1/2}$, curve b, characteristics of an MGM device with film thicknesses 270 nm.

It was observed during the measurements that the reported I-V characteristics were reproducible when counter electrode was biased with either polarity. This indicated that the metal-glass interfaces at bottom and top electrodes were identical in nature.

The results shown in figure 2 need to be carefully analysed, to identify the predominant conduction mechanism, since different types of conduction mechanisms can give rise to non-linear characteristics. One can first explain observed non-linearity in terms of Richardson-Schottky[7] or Poole-Frenkel[8] type of conduction mechanisms. Schottky emission occurs due to thermal activation of electrons over the metal-insulator or metal-semiconductor interface barrier because of lowering of barrier height due to the applied field. The Poole-Frenkel effect is basically similar to the Schottky effect, except that it is applied to thermal excitation of

electrons from traps into the conduction band of the insulator. In both the cases $\log I$ vs. $v^{1/2}$ characteristics are expected to be linear in nature. In Fig. 2 the curve 'b', shows $\log I$ vs. $v^{1/2}$ characteristics of a typical representative sample with film thickness 270 nm. It is seen that the characteristic curve is still non-linear in nature, which rules out the possibility of existence of Richardson Schottky or Poole-Frenkel as possible conduction mechanisms.

The other conduction mechanism, which gives rise to a highly non-linear I-V characteristics, is the space-charge-limited conduction (SCLC)[9], which is influenced by the traps. However, the exact nature of the traps present in the material under study depends on the type of the traps and their position with respect to the Fermi-level. It is therefore, necessary to apply this theory very carefully to explain the experimental results. In case of SCLC process the detailed features of the non-linear I - V characteristics are revealed in $\log I - \log V$ plot. Fig. 3 shows logarithmic plot of the I - V characteristics of the devices with different film thicknesses. It is observed that, the current flowing through the device decreases with increase in film thickness. However, the natures of the curves remain the same. It is seen that the characteristics are distributed in four regions (marked AB, BC, CD and DE) having different slopes, which implies that the I - V relation is of the type $I \propto V^n$ where n is the slope of the curve.

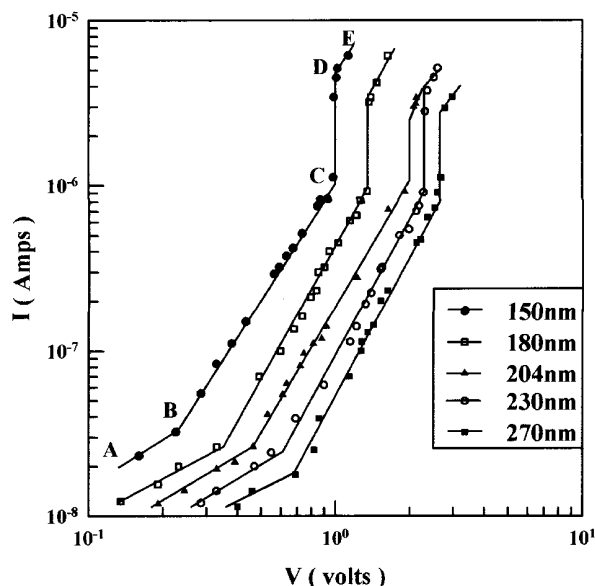


Figure 3. Log I - log V characteristics of the devices with different film thicknesses at 294 K.

For very low voltages (i.e. curve AB) the slope is equal to unity indicating that the conduction mechanism is Ohmic in the first region. This also indicates

that in this region the current is directly proportional to the applied voltage.

In the region 2, curve BC, the value of exponent n is found to be nearly equal to 2.5. This region starts at a particular voltage, V_x , which is the end of the first region. Thus, at V_x , the conduction mechanism is both Ohmic and SCLC. It is also noted from the Fig. 3 that V_x increases as thickness increases.

In the third region, curve CD, the slope increases to the value much larger than 2. This region is almost parallel to the current axis, indicating that the current - voltage relation follows a much higher power law. The transition voltage from second region to the third region is denoted by VTFL, which increases as thickness increases.

In the region 4, curve DE, the exponent is again found to be 2, indicating a trap filled SCLC process.

It is also noticed that the slopes of all the regions are independent of these film thickness.

Fig. 4 shows the $\log I - \log V$ characteristics at five different temperatures of a typical representative sample of film thickness 270 nm. It is seen that the nature of the curves is essentially same as that, in Fig. 3. It is also seen that as the temperature increases current through the device increases but V_x and VTFL decrease.

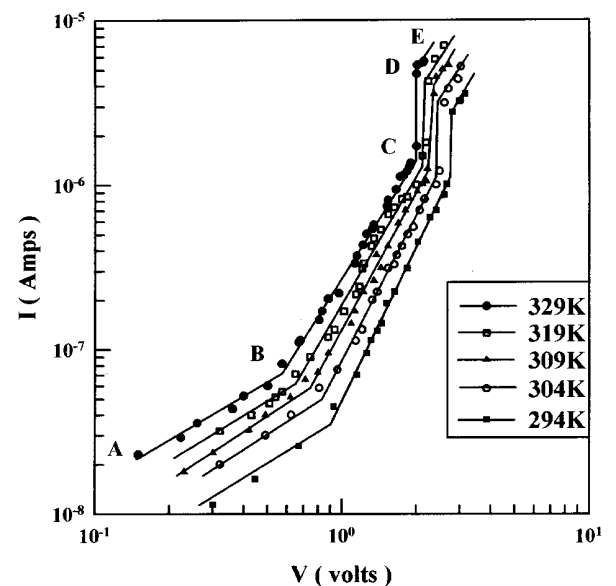


Figure 4. Log I - log V characteristics of the devices with thickness 270 nm at different temperatures.

It is also noticed that the slopes of the curves in region BC are temperature dependent such that as temperature increases the slopes decrease slightly; but the slopes of regions AB, CD and DE are practically independent of temperature.

These characteristic features of the I-V curves suggest that the conduction of the charge carriers in the

MGM devices under present study is governed by the SCLC mechanism. Therefore, the results of the measurements on the devices with various glass thicknesses and temperatures are analysed on similar lines and are shown to be consistent with the SCLC mechanism.

Since vacuum evaporated films tend to be a mixture of amorphous and crystalline regions, one can expect a large concentration of traps distributed in the energy band-gap [10]. Therefore, the SCLC phenomenon appropriate to such distribution can be applied to describe the conduction in these films. As the exact distribution of traps is difficult to predict, an approximations to the real distribution was attempted.

The Figs. 3 and 4 show that the I-V characteristics are governed by the relation $I \propto V^{-n}$. Also the plot shows two distinct cross-over voltages, V_x representing transition from Ohmic conduction to the SCLC with traps, and the V_{TFL} , which is transition from SCLC with traps to the trap filling level. This implies that the traps, in the present case, are situated at energy level higher than that of the Fermi-level of the material. Hence traps are expected to behave like donors [11]. Also, the temperature dependence of the region suggests a possibility of exponential distribution of traps.

Lampert has shown [9] that the current density in the second region is given by,

$$J = \left(\frac{9}{8}\right) \times (\mu K \epsilon_0 \theta) \times \left(\frac{V^2}{S^3}\right) \quad (1)$$

where

J = current density in the second region

K = dielectric constant of the material

ϵ_0 = permittivity of free space

θ = ratio of free charge carriers to the trapped carriers

S = thickness of the film

μ = mobility of the carriers

V = applied bias

Eq. (1) suggests that to establish the existence of SCLC a plot of log I versus log S should yield a straight line with slope equal to -3. The curve 'a' in Fig. 5 shows log I - log S curve generated using data of Fig. 3 corresponding to a constant voltage bias of 0.8V. It is seen that this plot is a straight line with slope equal to -3.2.

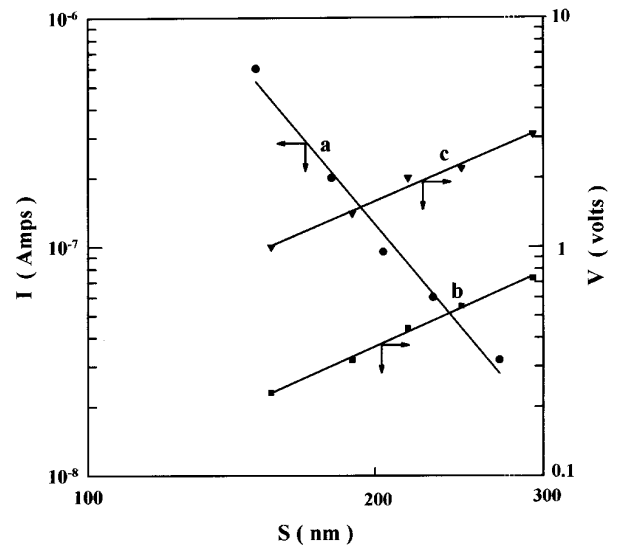


Figure 5. Curve a: Log I - log S characteristics of the devices. Curve b: Log V_x - log S characteristics of the devices. Curve c: Log V_{TFL} - log S characteristics of the devices. Temperature of the device = 294 K.

The transition voltages, V_x and V_{TFL} , transition from Ohmic region to the conduction with traps and transition from conduction with traps to the trap free conduction respectively, are given by,

$$V_x = \left(\frac{8}{9}\right) \times \left(\frac{en_0}{\theta}\right) \times S^2 \quad (2)$$

$$V_{TFL} = \frac{\epsilon Q_{TFL} S}{C} = \left(\frac{\epsilon Q_{TFL}}{AK\epsilon_0}\right) \times S^2 \quad (3)$$

where

Q_{TFL} = charge carriers injected at V_{TFL}

e = electronic charge

C = capacitance at V_{TFL}

A = area of the device

n_0 = free carrier density

Eqs. 2 and 3 suggest that the plots of log V_x versus log S and log V_{TFL} versus log S should yield straight lines with slope 2. Fig. 5, curve 'b' gives log V_x - log S curve, while curve 'c' gives log V_{TFL} versus log S plot. The slopes of the curves b and c are respectively, 2.17 and 1.97 which provide additional support for the existence of SCL conduction.

The temperature dependence of the current density, J , in the second region is given by [11],

$$j = en_0 \mu F \exp\left(\frac{F \epsilon_0 K}{e N_t k T S}\right) \quad (4)$$

where

F = electric field = $\frac{V}{S}$

N_t = trap density

Eq. 4 can be rewritten as,

$$\frac{J}{V} = \left(\frac{en_0\mu}{S}\right) \times \exp\left(\frac{V\epsilon_0K}{eN_tkTS^2}\right) \quad (5)$$

$$\therefore \frac{J}{V} = A_0 \exp\left(\frac{V}{V_0}\right) \quad (6)$$

with

$$A_0 = \frac{en_0\mu}{S} \quad (7)$$

$$V_0 = \frac{eN_tkTS^2}{\epsilon_0K} \quad (8)$$

Thus, a plot of $\log(I/V)$ versus V should yield a straight line with slope $(1/V_0)$ and intercept A_0 . Fig. 6 shows the $\log(I/V)$ versus V plots, generated using the data of Fig. 3, for the samples with different film thicknesses. Fig. 7 shows similar plots, for various temperatures generated using data of Fig. 4. It is seen that, while the slopes of the curves in the Fig. 6 remain the same, they decrease slightly with increase in temperature, as revealed from Fig. 7. The decrease in slope $(1/V_0)$ with temperature implies that the Rose model, [12] which predicts the nature of trap distribution can be applied in the present case. Using Eq. 7 and intercepts of plots in Figs. 6 and 7, trap densities for various film thicknesses and temperatures are computed. These values are shown in table 1a and 1b respectively. It is seen that the trap densities of the order of $10^{23} \text{ m}^{-3}\text{eV}^{-1}$ exist for the present system. These values are in close agreement with those reported for the similar disorder materials.[13,14] For highly disordered material the magnitude of trap density is as high as $10^{27} \text{ m}^{-3}\text{eV}^{-1}$ has been observed for vacuum deposited CdS films.[15]

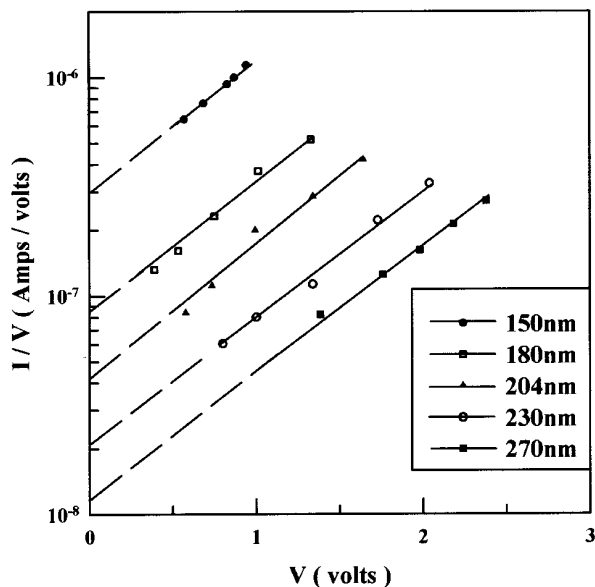


Figure 6. Log (I/V) - V characteristics of the devices with different film thicknesses at 294 K.

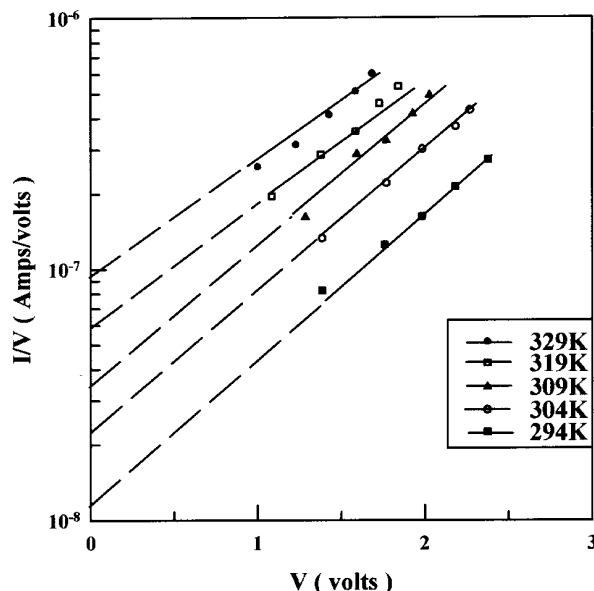


Figure 7. Log (I/V) - V characteristics of the devices at different temperatures, film thickness = 270 nm.

Table 1. Variation of trap density with thickness, table (a), and temperature, table (b).

(a)

Temperature = 294 K	
Thickness nm	$N_t(\text{m}^{-3}\text{eV}^{-1})$ $\times 10^{23}$
150	6.299
108	4.374
204	3.405
230	2.679
270	1.944

(b)

Thickness = 270 nm	
Temperature K	$N_t(\text{m}^{-3}\text{eV}^{-1})$ $\times 10^{23}$
294	1.944
304	1.640
309	1.347
319	1.172
329	1.055

It is further seen that using equation 7 and the intercepts the values for $n_0\mu$ can be calculated from the intercepts. The intercept, $\log A_0$, is also found to be a function of the mobility μ of carriers, free electron density and the thickness of the device. The mobility of carriers in glassy materials exhibits a trap activated temperature relation of the form [16],

$$\mu = \mu_0 \exp\left(\frac{E_t}{kT}\right) \quad (9)$$

where E_t is the activation energy of the traps

Eq. (9) can be rewritten as

$$n_0\mu = n_0\mu_0 \exp\left(\frac{E_t}{kT}\right) \quad (10)$$

Thus, it is possible to extract information about the activation energy of the traps by plotting $\log n_0\mu$ versus $1/T$ (Fig. 8). It is seen that the plot is linear and, from the slope, the value of E_t is calculated to be 0.48eV, which is the activation energy of traps. This value is in close agreement with the reported one for similar type of chalcogenide materials [17].

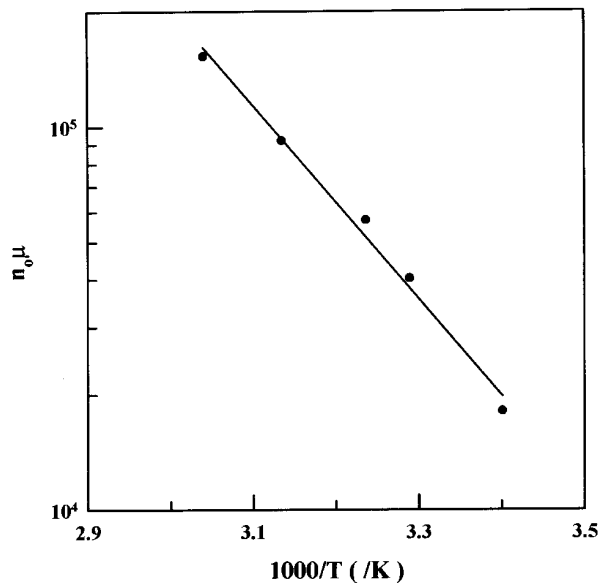


Figure 8. $\log(n_0\mu) - (1/T)$ characteristics of the device with film thickness 270 nm.

The distribution of the traps in the device could be either discrete or exponential. Rose [12] gives the current voltage relation, which is in the form $I \propto V^{[(Tc/T)+1]}$, where Tc is the characteristic temperature. Thus $[(Tc/T) + 1]$ is the slope of the second region of Fig. 3 which gives Tc as 600 K. Thus, kTc becomes 0.05eV, which is very small compared to the average activation energy of the traps determined as 0.48eV. This suggests that the distribution of traps is uniform which is expected for amorphous or polycrystalline films [12]

IV Conclusions

In this paper low field DC characteristics of the MGM devices are analysed. The dominant conduction mecha-

nism is identified as SCLC process. It is further showed that the traps are distributed uniformly in the forbidden band-gap. The activation energy of the traps is estimated as 0.48 eV. The trap density is found to decrease for increase in both the film thickness and the temperature.

Acknowledgement

The authors wish to thank Prof A.P. Sathe, for stimulating discussions and for critically reading the manuscript.

References

- [1] L. Kasturi, *Thin Film Phenomena*, McGraw-Hill Book Company.
- [2] N.F. Mott and E.A. Davis, *Electronic Process In Non-crystalline Materials*, Clarendon Press, Oxford 2nd edition (1978).
- [3] G.S. Nadkarni and V.S. Shirodkar, *Thin Solid Films* **105**, 115 (1983).
- [4] V.K. Dhavan, A. Mansingh and M. Sayer, *J. Non-crystalline Solids* **51**, 87 (1982).
- [5] K. Nassau and D.W. Murphy, *J. Non-crystalline Solids* **44**, 297 (1981).
- [6] A. Servini and A.K. Jonscher, *Thin Solid Films* **3**, 341 (1965).
- [7] W.Z. Schottky, *Phys.* **15**, 872 (1914).
- [8] Frenkel, *J. Phys. Rev.* **54**, 647 (1938).
- [9] M.A. Lampert, RCA Tech. Report No. PTR., p 1445 (1963).
- [10] J.G. Simmon, *J. Phys. D4*, 613 (1971).
- [11] M.A. Lampert and P. Mark, *Current injections in solids*, NY. Lond. (1970).
- [12] A. Rose, *Phys. Rev.* **97**, 1538 (1955).
- [13] S.P. Bodhane and V.S. Shirodkar, *J. Apply. Poly. Sci.* In press (Publication no. 6700).
- [14] T. Budinas, P. Mackus, A. Smilga, J. Vivvakas, *Phys. Sol. Stat.* **31**, 375 (1969).
- [15] J. Dresner and F.V. Shallcross, *Sol. Stat. Electr.* **5**, 205 (1962).
- [16] I. Solomon, R. Benferhat and H. Tran-Quoc, *Phys. Rev. B* **30**, 3422 (1984).
- [17] N. Kenshiro and C.K. Kwan *Jpn. Appl. Phys.* **18**, 1161 (1979).